

MORPHOLOGY AND MOLECULAR CHARACTERIZATION OF A NEW SPECIES OF THECATE BENTHIC DINOFLAGELLATE, *COOLIA MALAYENSIS* SP. NOV. (DINOPHYCEAE)¹

Chui-Pin Leaw²

Institute of Biodiversity and Environmental Conservation, Universiti Malaysia Sarawak, Kota Samarahan, 94300 Sarawak, Malaysia

Po-Teen Lim

Faculty of Resource Science and Technology, Universiti Malaysia Sarawak, Kota Samarahan, 94300 Sarawak, Malaysia

Kok-Wah Cheng, Boon-Koon Ng, and Gires Usup

Faculty of Science and Technology, Universiti Kebangsaan Malaysia, Bangi, 43600 Selangor, Malaysia

Coolia Meunier is an important component of benthic dinoflagellate assemblages in tropical and subtropical seas. In this study, detailed morphological observation of *Coolia* species from Malaysian waters was carried out using light and electron microscopy in parallel with molecular characterization of nuclear-encoded partial LSU rDNA, and internal transcribed spacer (ITS) regions. Live specimens were collected from seaweed samples and established into clonal cultures. There are significant morphological variations between the Malaysian isolates in comparison to the type species, *C. monotis* Meunier. The feature that differentiates the new species is the third postcingular plate (3^{'''}), which is the largest hypothecal plate in the Malaysian isolates, whereas in *C. monotis*, the 3^{'''} and 4^{'''} plates are almost equal in size. Detailed observations of the thecal pores also revealed the presence of fine perforations within the pores of the Malaysian isolates, but these perforations are absent in *C. monotis*. Comparisons between Malaysian isolates and *C. monotis* nucleotide sequence of the ITS region showed high genetic divergence at 28%, in contrast to the 0.3%–3% divergence observed among populations of the same species. Structural comparison of the second internal transcribed spacer (ITS2) rRNA transcript between the two species showed compensatory base changes (CBCs) in the three helices of ITS2 rRNA. Based on morphological and molecular data, the Malaysian isolates are considered to represent a new species, for which the name *Coolia malayensis* is proposed.

Key index words: benthic dinoflagellates; *Coolia malayensis*; ITS2 rRNA transcript; morphology; phylogeny

Abbreviations: CBC, compensatory base change; ITS, internal transcribed spacer

Benthic marine dinoflagellates are species that live attached to sand particles, corals, seaweeds, and mangroves. Many benthic dinoflagellates are capable of producing bioactive compounds, including those that can cause seafood toxicity. The most well-known human intoxication due to benthic dinoflagellates is ciguatera fish poisoning (CFP) where the responsible toxins occur in species of the genus *Gambierdiscus*. *Coolia* species often share the same habitats with other toxic epi-benthic dinoflagellates, and it has been suggested that the benthic dinoflagellate assemblage may contribute to CFP in ciguatera endemic areas (Tindall and Morton 1998).

The genus *Coolia* was originally described by Meunier (1919) with a single species, *C. monotis*, based on specimens collected from Nieuport, Belgium. *C. monotis* was subsequently collected and described by other researchers over the last few decades from wide geographic ranges and highly varied habitats (Lebour 1925, Balech 1956, Taylor 1979, Fukuyo 1981, Besada et al. 1982, Dodge 1982, Carlson and Tindall 1985, Faust 1992).

Coolia remained monospecific until *C. tropicalis* M. A. Faust (Faust 1995); *C. areolata* Ten-Hage, Turquet, Quod et Couté (Ten-Hage et al. 2000); and, most recently, *C. canariensis* S. Fraga (Fraga et al. 2008) were described. These additional species are differentiated by thecal plate arrangement and ornamentation. Recently, molecular phylogenetic analyses have been widely applied in species recognition and delineation of *Coolia* (Penna et al. 2005, Dolapsakis et al. 2006). Phylogenetic analyses of rRNA genes revealed and confirmed the status and identity of European *C. monotis* (Penna et al. 2005), and *C. canariensis* as a new species (Fraga et al. 2008). Considerable morphological variability has been reported in *C. monotis*, while analyses of molecular markers have revealed genetic divergences among *C. monotis* isolates from a wide geographic range (Penna et al. 2005, Dolapsakis et al. 2006). The cosmopolitan *C. monotis*, therefore, may comprise a complex of cryptic taxa.

¹Received 9 November 2008. Accepted 19 August 2009.

²Author for correspondence: e-mail cpleaw@ibec.unimas.my, chuipinl@yahoo.com.

Species delineation by traditional morphology-based taxonomy often presents challenges and provokes debate in dinoflagellate systematics. In an attempt to overcome the limitations of using morphological criteria alone to delineate species boundaries, researchers now incorporate more comprehensive integrated approaches, such as molecular and physiological criteria. Recently, the ITS2 of rRNA gene has been suggested as a suitable molecular marker to distinguish between closely related species (Müller et al. 2007). Müller et al. (2007) surveyed a vast majority of eukaryotes and showed that CBCs occurring in the secondary structures of ITS2 rRNA transcript between two organisms/species provide useful biological information at high taxonomic levels, and that this could be correlated with interspecies sexual incompatibility (Coleman 2003, 2007). Two taxa with even a single CBC in the relatively conserved paired region of ITS2 transcript are sexually incompatible and are thus biologically distinct according to the biological species concept (Coleman 2009). Studies of different molecular markers and analyses of mating compatibility among the *Pseudonitzschia pseudodelicatissima* species complex had proved the usefulness of ITS2 transcript in delineating the biological species concept (Amato et al. 2007, Amato and Montresor 2008).

In this study, we analyzed morphological and genetic characters of *Coolia* isolates from Malaysia in comparison to other previously described species in the genus. Both morphological and molecular data indicated that the Malaysian isolates differ significantly from *Coolia* species that have been described to date, and as such, a new species, *Coolia malayensis*, is here proposed.

MATERIALS AND METHODS

Samples. Seaweeds, coral fragments, seagrasses, and sand were collected by snorkeling or SCUBA. Sampling was carried out in Kota Kinabalu (05°59' N, 116°04' E), Port Dickson (02°31' N, 101°48' E), and Langkawi Island (06°20' N, 99°50' E). Samples were placed in separate plastic bags while still underwater, to which was added a little seawater. In the laboratory, the samples were shaken vigorously to dislodge attached dinoflagellate cells. The suspension was then passed through a handmade 120 µm mesh sieve to remove large debris. The material that passed through was sieved again with a handmade 20 µm mesh sieve. Material retained by the fine sieve was resuspended in sterile filtered seawater and examined under a stereoscope (Olympus stereomicroscope; Olympus, Tokyo, Japan) for cell isolation by micropipetting. Clonal cultures were established in ES-DK medium (Kokinis and Anderson 1995) with a salinity of 30 psu and maintained at 26°C under a 14:10 light:dark (L:D) photoperiod (Table S1 in the supplementary material).

Species identification. For LM, wild and cultured cells were examined with an Olympus BX51 microscope (Olympus, Melville, NY, USA) with a ×40 dry lens, N.A. 0.65. Digital images were captured with a Colorview F12 cooled CCD camera (Soft Imaging System GmbH, Hamburg, Germany). For epifluorescent images, cells were stained with 1% Calcofluor White M2R (Sigma, St. Louis, MO, USA) and examined under ultraviolet light with a UV filter set.

For SEM, cells were initially fixed with 4% glutaraldehyde for 1 h and postfixed with 1% osmium tetroxide for 0.5–1 h at room temperature. Cells were rinsed three times with dH₂O to remove salt and fixatives, dehydrated in a graded series of ethyl alcohol concentration, filter-mounted to a stub, and dried in a critical-point dryer. The sample was coated with gold using a Bio-Rad SC500 sputter coater (Bio-Rad, Hemel Hempstead, UK) and observed with a Philips XL30 scanning electron microscope (Philips Co., Eindhoven, the Netherlands). Average cell dimensions were calculated from measurements made on 20 cells.

DNA extraction, amplification, and sequencing of rDNA. Protocols for DNA extraction, PCR amplification, and sequencing were as previously described (Leaw et al. 2001). Briefly, cells were harvested from midexponential batch culture by centrifugation and then resuspended in NET lysis buffer (1% SDS, 15 mM NaCl, 10 mM EDTA, pH 8.0, and 10 mM Tris-HCl, pH 7.5) followed by cetyltrimethylammonium bromide (C-TAB) extraction. The mixture was extracted once with chloroform:isoamyl alcohol (C:I; 24:1) and followed standard phenol/chloroform procedures. DNA was precipitated by ethanol and sodium acetate (pH 5.0). The DNA pellet was then dissolved in TE buffer (pH 8.0).

Amplification and sequencing of rRNA genes (rDNA) were carried out as previously reported (Leaw et al. 2001, 2005). The ITS and 5.8S regions were amplified with the primers originally developed by Adachi et al. (1996) and modified by Leaw et al. (2001). The D1/D2 region of 28S rDNA was amplified with primer pairs D1R and D2C (Scholin et al. 1994). Sequencing was carried out using an ABI 377 automated sequencer (PE Applied Biosystems, Foster City, CA, USA). Sequencing for each sample was carried out for both strands. The sequences were deposited in GenBank and are listed in Table S1.

Secondary structure prediction. Secondary structure of 5.8S rRNA and its interaction with 28S rRNA was predicted for *Coolia* using RNAviz (De Rijk et al. 2003) with *Prorocentrum micans* as a model structure (Van der Auwera and De Wachter 1998). The secondary structure of the 5.8S–28S rRNA binary complex was then used to determine the ITS2 region by identifying the bordering sequences of 5.8S–28S rRNA junction. The secondary structure of the ITS2 rRNA transcript was folded, corrected manually, and viewed using Pseudoviewer 3 (Byun and Han 2006).

The ITS2 rRNA of strain CmPL01 was used as a template for homology modeling. Homology modeling was performed with identity matrix and 50% threshold for helix transfer using the ITS2-Database (Selig et al. 2008). ITS2 sequences of four strains of *C. monotis* retrieved from GenBank (AJ514919, AJ308524, AJ279032, and AJ319578) were used as comparative taxa.

Sequence alignment and phylogenetic reconstruction. The sequences obtained were aligned using Clustal-X (Thompson et al. 1997) and Bioedit version 6.0.7 (Hall 1999), while 4SALE (Seibel et al. 2006) was used for sequence-structure alignment. Sequence divergences were analyzed using DnaSP ver. 3.0 (DNA sequence polymorphism; Rozas and Rozas 1999).

For phylogenetic inference, alignment of LSU rDNA sequences obtained from Malaysian isolates of *Coolia* CmPL01 and other *Coolia* sequences (Table S1) was tested for the best model of nucleotide substitution using the Akaike information criterion (AIC) of Modeltest (Posada and Crandall 1998). Maximum-likelihood (ML) and maximum-parsimony (MP) analyses were carried out using PAUP* ver. 4.0b10 (Swofford 1998). ML analysis was performed with a heuristic search and tree-bisection-reconnection (TBR) swap with the following PAUP block: Lset Base = (0.2992 0.1563 0.2208) Nst = 6 Rmat = (1.0911 1.8894 0.5604 0.5455 3.2231) Rates = gamma Shape = 1.0009 Pinvar = 0. One hundred and 1,000 bootstrap (BS) replicates were generated for the MP and ML analyses,

respectively. A Bayesian analysis (BI) was carried out with MrBayes 3 (Huelsenbeck and Ronquist 2001) using a general-time-reversible (GTR) substitution model. Four simultaneous Markov chain Monte Carlo (MCMC) chains of 1×10^6 generations each were run, and trees were sampled every 100 generations. The posterior probabilities (PP) were estimated from the last 7,500 trees, and a majority-rule consensus tree was then constructed from the trees.

RESULTS

Coolia malayensis Leaw, P.-T. Lim et Usup sp. nov.

Description: Cellulae rotundis, 28–33 μm longae, 27–32 μm latae. Formula laminarum Po, 3', 7'', 6(c), 6?(s), 5''', 2'''. Patellae thecalis laevis, poris rotundis ad ovales tectis, poris 0.3 μm diametro mediocris porus maior poris minutis (0.05 μm diametro mediocris) in radialis ordinates penitus. Porus apicibus 5 μm longus. Patella apicalis singuli angustus, oblongus. Patella sexies precingularibus patellae in epithecum latissimus. Patella ter precingularibus patellae in hypothecam latissimus ad hypothecam medius

dorsalis occupans. Nucleus locatus in dorsalis hypotheca. Cellulae photosyntheticae. Numerus acc. GenBank (regio ITS): AF244945.

Cells round with length of 28–33 μm and width of 27–32 μm . Thecal plate formula: Po, 3', 7'', 6(c), 6?(s), 5''', 2'''. Theca plates smooth with round to oval pores with average diameter of 0.3 μm . Plates with radially arranged minute perforations of 0.05 μm average diameter located inside the pores. Apical pore 5 μm long. First apical plate 1' narrow and oblong. Sixth precingular plate 6'' the widest plate in the epitheca. Third postcingular plate 3''' the widest plate in the hypotheca, occupying mid-dorsal of the hypotheca. Nucleus located in the dorsal part of the hypotheca. Cells photosynthetic. GenBank accession number of ITS region: AF244945.

Type locality: Kota Kinabalu, (05°59' N, 116°04' E), Sabah, Malaysia, South China Sea.

Holotype: Figure 1 obtained from strain CmSA01. The strain is deposited in the Microalgae Culture Collection of Universiti Kebangsaan Malaysia.

Etymology: The epithet *malayensis* refers to Malaya.

Additional specimens examined: Langkawi Island (06°20' N, 99°50' E) and Port Dickson (02°31' N, 101°48' E) Malaysia, the Straits of Malacca.

Morphology. *C. malayensis* cells are round when observed in dorsoventral (Fig. 3A) and lateral view (Figs. 2A and 3B). Cells are small, 28–33 μm in length ($30.42 \pm 2.65 \mu\text{m}$, $n = 20$, mean \pm SD) and 27–32 μm in width ($29.77 \pm 2.40 \mu\text{m}$, $n = 20$). The thecal surface is smooth (Figs. 3, 4), irregularly scattered with round to oval large pores (average diameter 0.3 μm). The inner part of the thecal pores have scattered, very fine perforations of $\sim 0.05 \mu\text{m}$ in diameter; three to eight perforations are present in each thecal pore (Fig. 4C).

Individual thecal plates are delineated by the faint sutures and smooth intercalaries (Fig. 3). The apical pore complex (APC) is short and relatively straight, contiguous to the first, second, and third apical plates (1', 2', and 3') (Figs. 3A and 4A). The narrow apical pore (Po) is located in the APC and is $\sim 5 \mu\text{m}$ long (Figs. 3A and 4A). The 3' is quadrangular, bordering the 1', 2' APC, 4'', and 6'' and does not touch the 5'' (Figs. 3A and 4A). The right margin of 1' plate is straight and adjoins the sixth

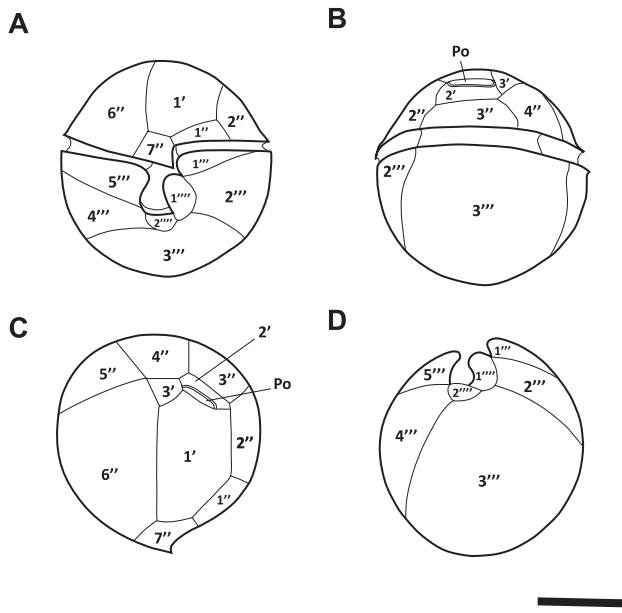


FIG. 1. Line illustration of *Coolia malayensis* sp. nov. (A) Ventral view. (B) Dorsal view. (C) Apical view. (D) Antapical view. Po, apical pore.

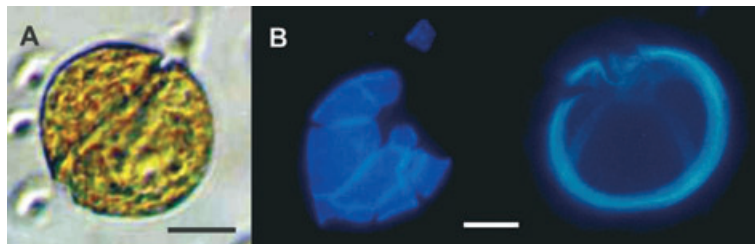


FIG. 2. *Coolia malayensis* sp. nov., LM. (A) Vegetative cell showing the yellow-brownish photosynthetic pigments and position of the nucleus (N). (B) Epi-fluorescence micrograph of the epitheca and hypotheca. Scale bars, 10 μm .

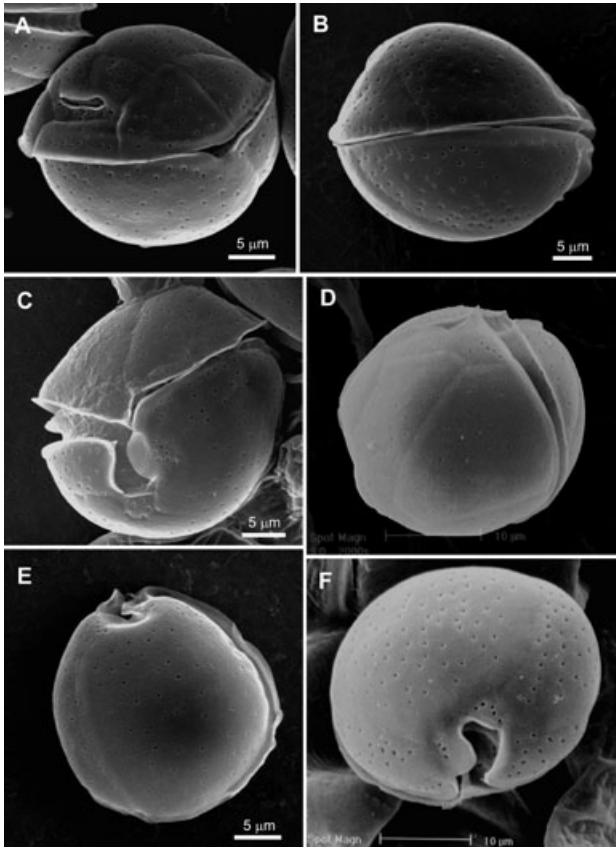


FIG. 3. *Coolia malayensis* sp. nov., SEM. (A) Cell in dorsoapical view showing the position of the apical pore complex (APC) and the apical pore (Po). (B) Cell in lateral view. (C) Ventral view of a cell showing a short sulcus surrounded by the sulcal lists. 1'''' and 2'''' are in contact and formed the posterior left edge of the sulcus. Note also the straight right margin of the 1'. (D) Ventroapical view showing the shape of 1' and the 6''. (E) Ventroantapical view showing the large 3''' occupying the middorsal of the hypotheca. (F) Antapical view of a cell showing the deep sulcus.

precingular plate (6''). The 1' is narrow and oblong (Fig. 3, C and D). The 6'' is the widest plate in the epitheca, occupying nearly half of the epitheca (Fig. 3D). The seventh precingular plate (7'') is

small, with a width-length ratio ranging from 1.2 to 1.5 (Fig. 3, C and D). The cingulum is narrow, descends by two cingulum widths, and is lined with two rows of marginal pores (Figs. 3, C and D; 4B).

In antapical view, the third postcingular plate (3''') is very wide, occupying the middorsal of the hypotheca. It is the widest plate in the hypotheca (Fig. 3, E and F). The first and second antapical plates (1'''' and 2''') are separated by the sulcus and in some cells do not touch each other. The sulcus is deep, short, and widely flared toward the antapex (Fig. 3, C, E, and F). Sulcal list extends from 5''' and is thin, covering the right part of the sulcus, while 1'''' bears a wide, developed left sulcal list. A narrow, almost straight list extends from 2'''' and is visible on the antapical side (Fig. 3F).

Distribution and ecology. *C. malayensis* was found at all the locations sampled in association with seaweeds and was particularly common in association with brown and red seaweeds, such as *Sargassum*, *Padina*, and *Turbinaria*. None was observed on green seaweeds examined or on seagrass, and very few were associated with coral fragments and sand. *C. malayensis* occurred concurrently with species of *Ostreopsis*, such as *O. ovata* and *O. lenticularis*. Specimens were also obtained from seaweeds that grew on nets used in fish cage cultures around Langkawi Island.

rDNA sequence information. GenBank accession numbers of the ITS1-5.8S-ITS2 rDNA (ITS region) sequences for *C. malayensis* are given in Table S1. The ITS region sequence lengths of all the strains were identical, with 111 nucleotides (nt) for ITS1, 154 nt for 5.8S rDNA, and 114 nt for ITS2. The GC content of ITS1 and ITS2 sequences was 29.7% and 28.9%, respectively.

The transcript folding pattern of the 5.8S-28S rRNA binary complex showed the 5.8S-5'LSU association (Fig. 5), from which can be defined the termini of the ITS2 region. The novel ITS2 rRNA transcript of *C. malayensis* had the typical four-helix structure (Fig. 6). The number of base pairs (bp) in the ITS2 structure was 36.

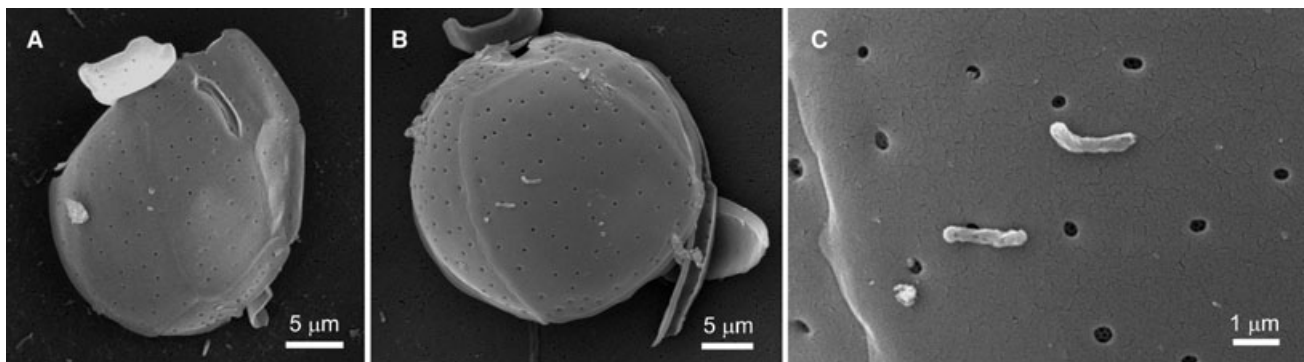


FIG. 4. *Coolia malayensis* sp. nov., SEM. (A) Squashed epitheca. (B) Squashed hypotheca. (C) Close-up of thecal pores showing fine perforations within pores.

For homology modeling, only a partial structure of *C. monotis* ITS2 (sequences retrieved from GenBank, Penna et al. 2005) encompassing three helices could be generated due to missing sequences at the 3' end of ITS2 sequences. Structural comparisons of the ITS2 rRNA between *C. malayensis* and *C. monotis* strains revealed some homologies in the three helices. Helix I was the most conserved, with at least 87% of structural elements transferred, whereas for helix II and III, the percent helix transfer ranged from 50% to 100% and 53% to 60%, respectively. CBCs as well as hemi-CBCs (HCBCs)

for the three helices ranged from four to six (Fig. 6).

Genetic divergence of ITS region within and between the two species of *Coolia* is summarized in Table 1. The degree of sequence divergence varied between the two species but remained low among the populations within the same species. In the region, the divergence estimated between *C. malayensis* and *C. monotis* was 28%. Within the three populations of *C. malayensis* isolates in Malaysia, the sequence divergences were in the range of 0.3%–0.6%, which was much lower than the 3% calculated

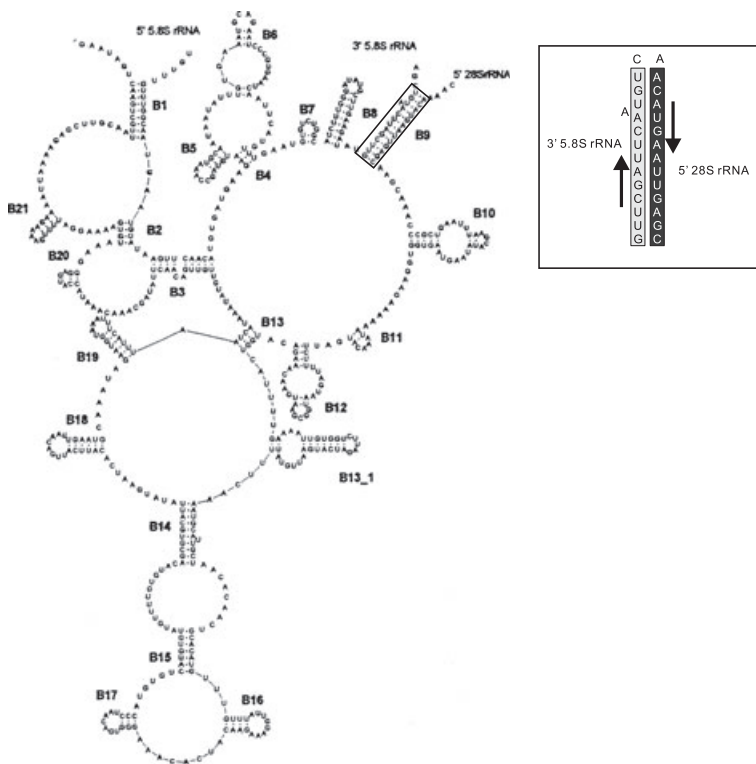


FIG. 5. A 5.8S–28S rRNA binary complex model of *Coolia malayensis* sp. nov. Inset: bordering sequence of tailing parts of the 28S and 5.8S rRNA (5.8S–5'LSU association) showing the end of the 5.8S (3') and start of the 28S (5') as indicated by arrows.

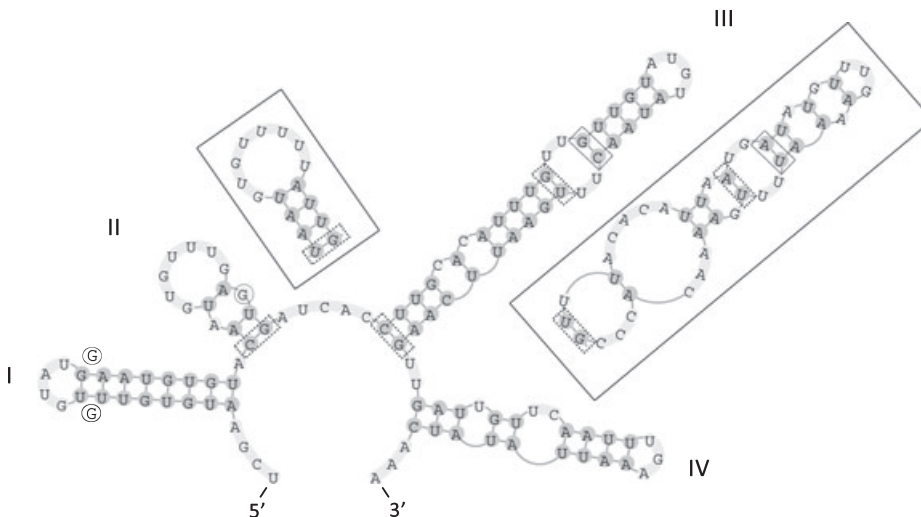


FIG. 6. ITS2 rRNA transcript secondary-structure model of *Coolia malayensis* sp. nov. The structure of ITS2 rRNA showed the typical four helices (I–IV). The base pairs in bolded line and dash boxes indicate compensatory base changes (CBCs) and hemi-compensatory base changes (HCBCs). Single base changes are indicated in circles, and boxes denote the changes of helix ends in comparison to *C. monotis* strain SZN 43 (AJ308524).

TABLE 1. Genetic distances in the nuclear noncoding internal transcribed spacers (ITS1 and ITS2) and 5.8S rDNA regions within and between *Coolia malayensis* sp. Nov. and *C. monotis*.

| Among populations of species | | | |
|--|--------------|----------------------|-------------------|
| <i>C. malayensis</i> sp. nov. | Port Dickson | Kota Kinabalu | Langkawi Island |
| Port Dickson ($n = 4$) | | 0.60 ± 0.33 | 0.33 ± 0.15 |
| Kota Kinabalu ($n = 2$) | 0.00409 | | 0.27 ± 0.27 |
| Langkawi Island ($n = 2$) | 0.00231 | 0.00267 | |
| <i>C. monotis</i> ^a | Atlantic | Mediterranean | |
| Atlantic ($n = 2$) | | 3.33 ± 1.78 | |
| Mediterranean ($n = 2$) | 0.02800 | | |
| Between species | | <i>C. malayensis</i> | <i>C. monotis</i> |
| <i>C. malayensis</i> ($n = 8$) | | | 28.11 ± 6.37 |
| <i>C. monotis</i> ^a ($n = 4$) | 0.11741 | | |

Molecular distances (p , Jukes and Cantor; upper diagonal) are expressed as percentage of the mean ± SD. Nucleotide diversities (P_i) are in the lower diagonal.

^aPenna et al. (2005).

for two populations of *C. monotis* from Europe (Table 2).

Phylogenetic analyses of available sequences for LSU rDNA (D1-D2) of *Coolia* (Table S1) were carried out using *O. lenticularis* OIPL01 (AF244941) as the outgroup. MP analysis of the aligned sequences showed a total of 713 characters (including gaps), of which 206 characters were constant, 411 variable characters were parsimony informative, and 96 characters were parsimony uninformative. Phylogenetic analyses yielded identical tree topologies by MP, ML, and BI. Here, only the BI tree is shown (Fig. 7). The resulting trees yielded four major end-clades, namely, clades I, II, III, and IV (Fig. 7). Clade I comprised a putative *C. monotis* strain from Belize (CCMP1744) and an undescribed *Coolia* species from Indonesia. *C. canariensis* grouped out as an individual clade (Clade II). The *C. malayensis* strain from Malaysia (CmPL01), in addition to two putative *C. monotis* strains from New Zealand (CAWD39) and Florida (CCMP1345) (Clade III), forms a sister taxon to Clade IV; Clade IV comprises the European strains of *C. monotis*. The individual clades were strongly supported by bootstrap values

from MP and ML analyses (100%), as well as BI posterior probabilities (1.00).

Sequence divergence of D1-D2 LSU rDNA gene for pair-wise comparison among clades is shown in Table 2. The average intraclade divergence ranges from 0.5 substitutions (within Clade III) up to 68.3 substitutions in Clade II. The interclade comparison revealed high divergences among the clades, with the lowest divergence of 16.7% (between Clades III and IV) to 63.1% (between Clades I and III).

DISCUSSION

Only a very small portion of Malaysia's marine waters have been sampled in this study, but even so, there is now evidence of the occurrence of potentially toxic benthic dinoflagellates at all locations sampled. One of the most common species found in the samples, which has been successfully cultured, is *C. malayensis*.

Comparison with other species of Coolia. Morphological examination of *C. malayensis* shows significant differences from other species of the genus, inferred from illustrations of the original descriptions (Fig. 8). The epithecal plate layout of *C. malayensis* is very similar to *C. monotis*, and *C. tropicalis*, but with some notable differences. The 1' of *C. malayensis* is practically akin to *C. monotis*, with straight left and right margins in the apical view, in contrast to the wedged-shaped 1' of *C. tropicalis* (Faust 1995, fig. 12) and beret-shaped 1' in *C. areolata* (Ten-Hage et al. 2000, fig. 10) and *C. canariensis* (Fraga et al. 2008, fig. 2). The 3' in *C. malayensis* appears quadrangular, differing from that of *C. monotis*, which is pentagonal, but similar to that of *C. tropicalis* (Faust 1995, fig. 7). *C. malayensis* also differs from others by its relatively few pores on the thecae (Table 3). Furthermore, the presence of radially arranged minute perforations within the theca pores in the spe-

TABLE 2. Genetic distances in the 691 unambiguously aligned base pairs of D1-D2 LSU rDNA regions of *Coolia* species.

| Clades | I | II | III | IV |
|--------|----------------|----------------|----------------|----------------|
| I | 0.01881 | 58.1 ± 24.6 | 63.1 ± 26.7 | 62.8 ± 15.8 |
| II | 0.25482 | 0.10928 | 60.4 ± 23.6 | 60.5 ± 13.3 |
| III | 0.23050 | 0.25097 | 0.00082 | 16.7 ± 3.7 |
| IV | 0.13709 | 0.17347 | 0.06384 | 0.00987 |

Molecular divergence (p , Jukes and Cantor; upper diagonal) is expressed as percentage of the mean ± SD. Nucleotide diversities (P_i) are in the lower diagonal. Intraclade comparisons of P_i are bolded. Refer to Figure 7 for definition of Clades I to IV.

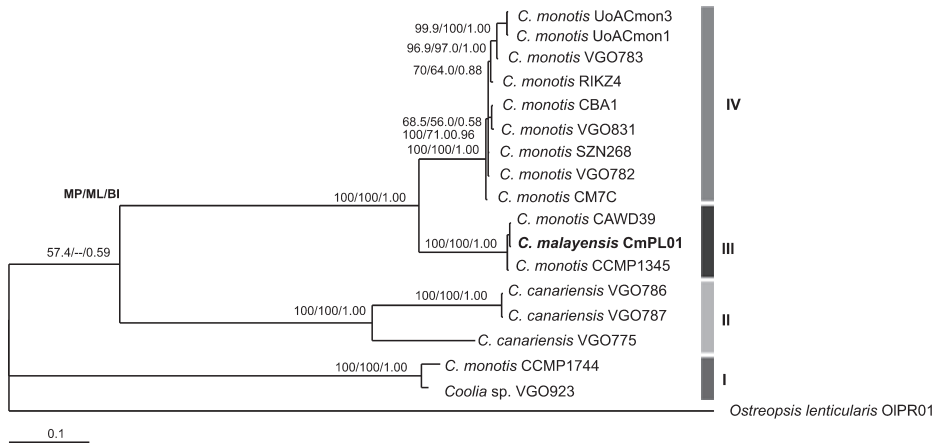


FIG. 7. Phylogenetic tree of *Coolia* species derived from Bayesian analysis of LSU rDNA (D1-D2) nucleotide sequences. Bayesian posterior probability (PP) values and percent parsimony and maximum-likelihood bootstrap supports (1,000 replications) are shown at the left of internal nodes. The LSU rDNA sequence from *C. malayensis* determined in this study is in boldface. The four end-clades have been labeled as Clades I, II, III, and IV for comparison.

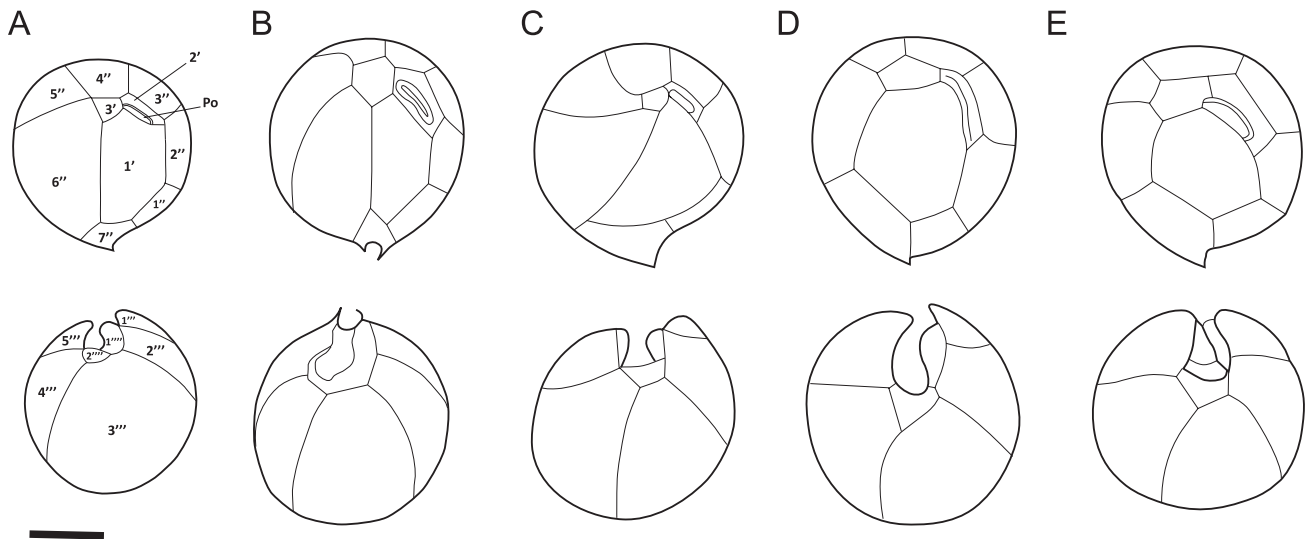


FIG. 8. Thecal plate tabulations of *Coolia* species based on original descriptions. Scale bar, 10 μ m. (A) *C. malayensis*. (B) *C. monotis* (redrawn from Meunier 1919). (C) *C. tropicalis* (redrawn from Faust 1995). (D) *C. areolata* (redrawn from Ten-Hage et al. 2000). (E) *C. canariensis* (redrawn from Fraga et al. 2008). Po, apical pore.

cies is noteworthy, which is different from *C. monotis* and the others where the thecal pores penetrate deeply into the thecal plates (Faust 1992, fig. 10; Faust 1995, fig. 11; Fraga et al. 2008, fig. 4d). The apical pore (Po) of *C. malayensis* is relatively short, in fact, the shortest among the species in the genus (Table 3).

Fraga et al. (2008) proposed a length-to-width ratio (L:W) of the seventh precingular plate 7'' to differentiate between *Coolia* species. The 7'' of *C. monotis* is very small, with an L:W ratio of ~ 1 . In *C. canariensis* and *C. areolata*, they are larger, with L:W ratio of ~ 2 . *C. tropicalis* had the largest plate, with an L:W ratio of ~ 4 . *C. malayensis* has slightly larger 7'' compared to *C. monotis*, with an L:W ratio ranging from 1.2 to 1.5 (Table 3).

Hypotheca plate characteristics have been considered as the most conservative characters after the cingular and sulcal plates (Balech 1980). In *C. malayensis*, there is a notable difference in the

hypotheca plates as compared with other *Coolia* species. The third postcingular plate (3''') of *C. malayensis* is broad and large, occupying the middorsal of the hypotheca, while in other species, both the 3''' and 4''' are about equal in size (Table 3, Fig. 8). This feature alone demonstrates that *C. malayensis* is different from the other species of *Coolia*.

Cells of *C. malayensis* are the smallest sized in the genus. According to Fukuyo (1981), two distinct types of *C. monotis* with two different cell-size ranges were observed by Yasumoto et al. (1980) in samples from French Polynesia. Moreover, the distinct size differences were maintained even after a few months in culture. However, the two types were considered the same species based upon thecal morphology. It remains uncertain whether those isolates were actually two cryptic species of *Coolia*.

Taxonomic incongruity. Morphological variability and plasticity in *Coolia* species, particularly *C. monotis*,

TABLE 3. Proposed diagnostic morphological characteristics of *Coolia* species.

| | <i>C. malayensis</i> | <i>C. monotis</i> ^{a,b,c} | <i>C. tropicalis</i> ^d | <i>C. areolata</i> ^e | <i>C. canariensis</i> ^f |
|--|--|---|---|--|--|
| Thecal surface ornamentation | Smooth | Smooth | Smooth | Areolated | Smooth, slightly arcolated in the hypotheca |
| Thecal pores | Oval to round with smooth edge, average diameter of 0.3 µm, 3–8 min perforations (~ 0.05 µm diam) inside each pore | Round pores with smooth edge | Round pores with smooth edge | Round pore with reticulation, average diameter of 0.2 µm | Round and oval pores with smooth edge in epitheca, slightly reticulated in hypotheca |
| Thecal pore density ^g | Few (<6) | Few (<4) ^{a,c} Very dense (>60) ^b | Moderate (<10) | Dense (17–25) | Moderate (6–8) |
| Apical pore plate (Po) | ~5 µm long | 10–12 µm long | ~7 µm long | 9–10 µm long | ~ 8 µm long |
| First apical plate (1') | Narrow and oblong, straight margin between 1' and 6'' | Oblong, straight margin between 1' and 6'' | Wedge shaped, displaced to the ventral left | Broad, margin between 1' and 6'' displaced to the right | Broad, margin between 1' and 6'' displaced to the right |
| Third apical plate (3''') | Quadrangular | Pentagonal ^{a,b} to partly wedge shaped ^c | Quadrangular | Pentagonal | Pentagonal |
| Length-to-width ratio of seventh precingular plate (7'') | 1.2–1.5 | ~ 1 | 4 | 2 | 2 |
| Widest epitheca plate | 6'' | 6'' | 1'' | 1'' | 1'' |
| Widest hypotheca plate | 3''' | 3''' and 4''' in almost equal size | 3''' and 4''' in almost equal size | 3''' and 4''' in almost equal size | 3''' and 4''' in almost equal size |
| Cell length (µm) | 21–31 | 26–50 | 23–40 | 30–36.5 | 27.2–38.4 |
| Cell width (µm) | 23–27 | 22–45 | 25–39 | 28–36.5 | 25.6–40.0 |

^aCompilation of Meunier (1919), Balech (1956), Fukuyo (1981), Dodge (1982).

^bFaust (1992).

^cDolapsakis et al. (2006).

^dFaust (1995).

^eTen-Hage et al. (2000).

^fFraga et al. (2008).

^gThecal pore densities are estimated from the number of pores per 25 µm² of thecal surface.

has been demonstrated by many researchers and suggested the presence of a complex of cryptic species. For example, Greek strains of *C. monotis* differ slightly from the type species specifically in the shape of 3' (Dolapsakis et al. 2006). The shape of 3' is pentagonal, but partly wedge shaped in the Greek strains, while in the type specimen, the plate is pentagonal (Meunier 1919, fig. 14; Balech 1956, fig. 53). Our analyses showed that the shape of 3' is variable and not concordant with the phylogenetic framework; therefore, reliability of the feature as a truly diagnostic trait is questionable.

Studies on *C. monotis* strains from New Zealand (Rhodes and Thomas 1997, Rhodes et al. 2000), basing their description solely on thecal plate shape, designated the isolates as *C. monotis* differentiated from *C. tropicalis* by the shape of 1'. In our analyses, we noted that the New Zealand strain (CAWD39) and the Florida strain (CCMP1345) are more closely related to *C. malayensis* (Fig. 7, Table 2). The strains are most probably *C. malayensis* based on our molecular analyses, but unfortunately, the species identity for the strains cannot be resolved because of insufficient morphological evidence.

C. monotis from Belize, described by Faust (1992), differs morphologically from the European *C. monotis*, as well as from *C. malayensis*, especially in the thecal pore density (Table 3; refer to Faust 1992, figs. 2–4). In the LSU rDNA analysis, a Belize strain (CCMP1744), putatively described as *C. monotis*, forms a paraphyletic clade separated from the European *C. monotis* (Fig. 7, Table 2). In accordance with Fraga et al. (2008), this Belize strain, together with an Indonesian strain (VGO923), may correspond to a further novel taxon.

Phylogenetic analysis using LSU rDNA sequence data demonstrates that *C. malayensis* is more closely related to *C. monotis* than to *C. canariensis*. This finding is consistent with morphological characteristics. Unfortunately, ITS and LSU sequences of some species of *Coolia* were not available for analysis; thus, the phylogenetic relationships among *Coolia* species remain unresolved. Evidence of the species status may be enhanced by revealing the cladal interrelationship; however, detailed morphological investigations would still be needed to clarify the taxonomic status of the French Polynesian, New Zealand, Belize, and Indonesian strains.

ITS2 transcript information. In addition to the morphological differences, and LSU rDNA-generated phylogeny, the results of structural comparisons of ITS rRNA transcript provided further evidence for the separation of *C. malayensis* from the other species of *Coolia*. The degree of sequence divergence in the ITS regions between *C. malayensis* and European *C. monotis* was similar to the 29% reported for the two species of *Ostreopsis*, namely, *O. ovata* and *O. cf. siamensis* (Penna et al. 2005). This is in contrast to values obtained when comparing the divergence within populations of either *C. malayensis* or *C. mono-*

tis, for which <3% sequence divergence was observed. Recently, Litaker et al. (2007) evaluated the usefulness of the ITS region as a unique species-specific “DNA barcode” in species recognition and proposed that a between-species uncorrected genetic distance in the region could be used to differentiate most dinoflagellate species. When comparing the divergence values within species of either *C. malayensis* or *C. monotis*, the intraspecific genetic distances were much lower than those observed between species. The within- and between-species variation observed in this study thus provided strong support for *C. malayensis* as a new species.

Previous studies have suggested that the ITS2 transcript is a reliable molecular classifier for delineating species or subspecies (Coleman 2003, 2007, Müller et al. 2007). Species distinction based on CBCs has been proved with >90% reliability at least for plants and fungi (Müller et al. 2007), although lack of CBCs between two taxa does not necessarily mean that they are the same species. In this study, structural comparison of *C. malayensis* and *C. monotis* showed marked differences in the ITS2 region. Comparison of the ITS2 rRNA transcript secondary structure showed one CBC and more than four HCBCs. Thus, it is proposed that the ITS2 secondary-structure information in this study is sufficient to conclude that *C. malayensis* and *C. monotis* are two distinct biological species. However, studies on mating compatibility of the two species are required to corroborate this conclusion. In future studies, it is suggested that ITS secondary structure be included in the molecular analyses to gain better phylogenetic resolution for *Coolia*.

We are grateful to the three anonymous reviewers for their constructive and helpful comments on earlier drafts. We thank Dr. Peter Boyce for Latin translation of the species diagnosis, his valuable suggestions, and English revision of the manuscript. This work was supported by the Malaysian Government through IRPA grants and UNIMAS short-term grants.

- Adachi, M., Sake, Y. & Ishida, Y. 1996. Analysis of *Alexandrium* (Dinophyceae) species using sequences of the 5.8S ribosomal DNA and internal transcribed spacer regions. *J. Phycol.* 32: 424–32.
- Amato, A., Kooistra, W. H. C. F., Ghiron, J. H. L., Mann, D. G., Pröschold, T. & Montresor, M. 2007. Reproductive isolation among sympatric cryptic species in marine diatoms. *Protist* 158:193–207.
- Amato, A. & Montresor, M. 2008. Morphology, phylogeny, and sexual cycle of *Pseudo-nitzschia mannii* sp. nov. (Bacillariophyceae): a pseudo-cryptic species within the *P. pseudodelicatissima* complex. *Phycologia* 47:487–97.
- Balech, E. 1956. Étude des dinoflagellés du sable de Roscoff. *Rev. Algol. (N. Ser.)* 2:29–52.
- Balech, E. 1980. On the thecal morphology of dinoflagellates with special emphasis on cingular and sulcal plates. *Ann. Centro Mar. Limnol. Univ. Natl. Autón. Mex.* 7:57–68.
- Besada, E. G., Loeblich, L. A. & Loeblich, A. R., III. 1982. Observations on tropical, benthic dinoflagellates from ciguatera-endemic areas: *Coolia*, *Gambierdiscus*, and *Ostreopsis*. *Bull. Mar. Sci.* 32:723–35.

- Byun, Y. & Han, K. 2006. PseudoViewer: web application and web service for visualizing RNA pseudoknots and secondary structures. *Nucleic Acids Res.* 34:416–22.
- Carlson, R. D. & Tindall, D. R. 1985. Distribution and periodicity of toxic dinoflagellates in the Virgin Islands. In Anderson, D. M., White, A. W. & Baden, D. G. [Eds.] *Toxic Dinoflagellates*. Elsevier Science Publ., New York, pp. 171–6.
- Coleman, A. W. 2003. ITS2 is a double-edged tool for eukaryote evolutionary comparisons. *Trends Genet.* 19:370–5.
- Coleman, A. W. 2007. Pan-eukaryote ITS2 homologies revealed by RNA secondary structure. *Nucleic Acids Res.* 35:3322–9.
- Coleman, A. W. 2009. Is there a molecular key to the level of “biological species” in eukaryotes? A DNA guide. *Mol. Phylogenet. Evol.* 50:197–203.
- De Rijk, P., Wuyts, J. & De Wachter, R. 2003. RnaViz2: an improved representation of RNA secondary structure. *Bioinformatics* 19:299–300.
- Dodge, J. D. 1982. *Marine Dinoflagellates of the British Isles*. Her Majesty's Stationery Office, London, 303 pp.
- Dolapsakis, N. P., Kilpatrick, M. W., Economou-Amilli, A. & Tafas, T. 2006. Morphology and rDNA phylogeny of a Mediterranean *Coolia monotis* (Dinophyceae) strain from Greece. *Sci. Mar.* 70:67–76.
- Faust, M. A. 1992. Observations on the morphology and sexual reproduction of *Coolia monotis* (Dinophyceae). *J. Phycol.* 28: 94–104.
- Faust, M. A. 1995. Observation of sand-swelling toxic dinoflagellates (Dinophyceae) from widely differing sites, including two new species. *J. Phycol.* 31:996–1003.
- Fraga, S., Penna, A., Bianconi, L., Paz, B. & Zapata, M. 2008. *Coolia canariensis* sp. nov. (Dinophyceae), a new nontoxic epiphytic benthic dinoflagellate from the Canary Islands. *J. Phycol.* 44:1060–70.
- Fukuyo, Y. 1981. Taxonomical study on benthic dinoflagellates collected in coral reefs. *Bull. Jpn. Soc. Sci. Fish.* 47:967–78.
- Hall, T. 1999. BioEdit: a user-friendly biological sequence alignment editor and analysis program for Windows 95/98/NT. *Nucleic Acids Symp. Ser.* 41:95–8.
- Huelsenbeck, J. P. & Ronquist, F. 2001. MRBAYES: Bayesian inference of phylogeny. *Bioinformatics* 17:754–5.
- Kokinos, J. P. & Anderson, D. M. 1995. Morphological development of resting cysts in cultures of the marine dinoflagellate *Lingulodinium polyedrum* (= *L. machaerophorum*). *Palynology* 19:143–66.
- Leaw, C. P., Lim, P. T., Ahmad, A. & Usup, G. 2001. Genetic diversity of *Ostreopsis ovata* (Dinophyceae) from Malaysia. *Mar. Biotechnol.* 3:246–55.
- Leaw, C. P., Lim, P. T., Ng, B. K., Cheah, M. Y., Ahmad, A. & Usup, G. 2005. Phylogenetic analysis of *Alexandrium* species and *Pyrodinium bahamense* (Dinophyceae) based on theca morphology and nuclear ribosomal gene sequence. *Phycologia* 44:550–65.
- Lebour, M. V. 1925. *The Dinoflagellates of the Northern Seas*. Marine Biological Association of UK, Plymouth, UK, 250 pp.
- Litaker, R. W., Vandersea, M. W., Kibler, S. R., Reece, K. S., Stokes, N. A., Lutzoni, F. M., Yonish, B. A., West, M. A., Black, M. N. D. & Tester, P. A. 2007. Recognizing dinoflagellate species using ITS rDNA sequences. *J. Phycol.* 43:344–55.
- Meunier, A. 1919. Microplancton de la Mer Flamande. 3. Les Péridiniens. *Mem. Mus. R. Hist. Nat. Bruxelles* 8:3–116.
- Müller, T., Philippi, N., Dandekar, T., Schultz, J. & Wolf, M. 2007. Distinguishing species. *RNA* 13:1469–72.
- Penna, A., Vila, M., Fraga, S., Giacobbe, M. G., Andreoni, F., Riobó, P. & Vernesi, C. 2005. Characterization of *Ostreopsis* and *Coolia* (Dinophyceae) isolates in the western Mediterranean Sea based on morphology, toxicity and internal transcribed spacer 5.8S rDNA sequences. *J. Phycol.* 41:212–25.
- Posada, D. & Crandall, K. A. 1998. Modeltest: testing the model of DNA substitution. *Bioinformatics* 14:817–8.
- Rhodes, L. L., Adamson, J., Suzuki, T., Briggs, L. & Garthwaite, I. 2000. Toxic marine epiphytic dinoflagellates, *Ostreopsis siamensis* and *Coolia monotis* (Dinophyceae), in New Zealand. *N. Z. J. Mar. Freshw. Res.* 34:371–83.
- Rhodes, L. L. & Thomas, A. E. 1997. *Coolia monotis* (Dinophyceae): a toxic epiphytic microalgal species found in New Zealand (Note). *N. Z. J. Mar. Freshw. Res.* 31:139–41.
- Rozas, J. & Rozas, R. 1999. DnaSP version 3: an integrated program for molecular population genetics and molecular evolution analysis. *Bioinformatics* 15:174–5.
- Scholin, C. A., Herzog, M., Sogin, M. & Anderson, D. M. 1994. Identification of group- and strain-specific genetic markers for globally distributed *Alexandrium* (Dinophyceae). II. Sequence analysis of a fragment of the LSU rRNA gene. *J. Phycol.* 30:999–1011.
- Seibel, P. N., Müller, T., Dandekar, T., Schultz, J. & Wolf, M. 2006. 4SALE – a tool for synchronous RNA sequence and secondary structure alignment and editing. *BMC Bioinformatics* 7:498.
- Selig, C., Wolf, M., Müller, T., Dandekar, T. & Schultz, J. 2008. The ITS2 Database II: homology modelling RNA structure for molecular systematics. *Nucleic Acids Res.* 36:377–80.
- Swofford, D. L. 1998. *PAUP*: Phylogenetic Analysis Using Parsimony (and Other Methods)*. Sinauer Associates, Sunderland, Massachusetts.
- Taylor, F. J. R. 1979. A description of the benthic dinoflagellate associated with maitotoxin and ciguatera, including observation on Hawaiian material. In Taylor, D. L. & Seliger, H. H. [Eds.] *Toxic Dinoflagellate Blooms, Developments in Marine Biology*, Vol. 1. Elsevier, North-Holland, Amsterdam, pp. 71–6.
- Ten-Hage, L., Turquet, J., Quod, J. P. & Couté, A. 2000. *Coolia areolata* sp. nov. (Dinophyceae), a new sand-dwelling dinoflagellate from the southwestern Indian Ocean. *Phycologia* 39:377–83.
- Thompson, J. D., Gibson, T. J., Plewniak, F., Jeanmougin, F. & Higgins, D. G. 1997. The CLUSTALX windows interface: flexible strategies for multiple sequence alignment aided by quality analysis tools. *Nucleic Acids Res.* 25:4876–82.
- Tindall, D. R. & Morton, S. L. 1998. Community dynamics and physiology of epiphytic/benthic dinoflagellates associated with ciguatera. In Anderson, D. M., Cembella, A. D. & Hallegraeff, G. M. [Eds.] *Physiological Ecology of Harmful Algal Blooms*. NATO ASI Series, Vol. G 41. Springer-Verlag, Berlin, pp. 293–314.
- Van der Auwera, G. & De Wachter, R. 1998. Structure of the large subunit rDNA from a diatom, and comparison between small and large subunit ribosomal RNA for studying stramenopile evolution. *J. Eukaryot. Microbiol.* 45:521–7.
- Yasumoto, T., Oshima, Y., Murakami, Y., Nakajima, I., Bagnis, R. & Fukuyo, Y. 1980. Toxicity of benthic dinoflagellates found in coral reef. *Bull. Jpn. Soc. Sci. Fish.* 46:327–31.

Supplementary Material

The following supplementary material is available for this article:

Table S1. *Coolia* species used in the study.

This material is available as part of the online article.

Please note: Wiley-Blackwell are not responsible for the content or functionality of any supplementary materials supplied by the authors. Any queries (other than missing material) should be directed to the corresponding author for the article.